End-to-End Dynamic Stability Modeling and Performance for Segmented Optical Telescopes

KEY FINDINGS OF SYSTEM LEVEL SEGMENTED TELESCOPE DESIGN (SLSTD) PHASE I STUDY

ExEP Colloquium, May 20, 2019

Larry Dewell, Alison Nordt

Ankur Chopra, Kia Tajdaran, Mike Jacoby, Torben Andersen, Clem Tillier

Lockheed Martin Advanced Technology Center, Palo Alto, CA

LOCKHEED MARTIN

Study Overview and Key Objectives

LOCKHEED MARTIN

* Develop a comprehensive integrated model of a segmented optical space telescope, including structural dynamics, control systems, segmented telescope optical sensitivities and realistic disturbance sources
* Quantify the dynamic errors of the architecture, particularly to support coronagraph performance
* Design a complete line-of-sight control system architecture for of the LUVOIR observatory that integrates a Fast Steering Mirror (FSM), LOS measurement derived from a payload science instrument , and a noncontact spacecraft-payload vibration isolation interface
- Perform integrated Structural Thermal Optical (STOP) modeling for HabEx and predict quasi-static Primary Mirror figure error due to variation in the operational thermal environment
- Assess the manufacturability and manufacturing processes of the key optical components

* **Scope of this presentation**

See full final report at: http://www.astrostrategictech.us/

External Partners:

- Collins Aerospace (ISR Systems)
- Harris Corporation (Space and Intelligent Systems)
- Coherent

STUDY OBJECTIVES FOCUSED ON FIRST-PRINCIPLES ANALYSIS, AND LEVERAGED TEAM EXPERTISE OF LARGE SPACE-BASED OPTICAL TELESCOPES

The LUVOIR 15-meter architecture and non-contact isolation

- The baseline LUVOIR architecture involves a non-contact vibration isolation and precision pointing (VIPPS) interface
- VIPPS enables the telescope to achieve extreme pointing and image stability while still meeting the line-of-sight agility requirements consistent with its astronomical Surveyor goals
- The payload controls overall payload attitude and telescope line-of-sight by pushing against the spacecraft inertia using a set of six non-contact voice coil actuators, while the spacecraft controls its inertial attitude such that interface stroke and gap are maintained
- Since the telescope is physically separated, the disturbances and structural excitation of the spacecraft and sunshield do not propagate to the telescope, enabling extreme stability across a broad frequency range

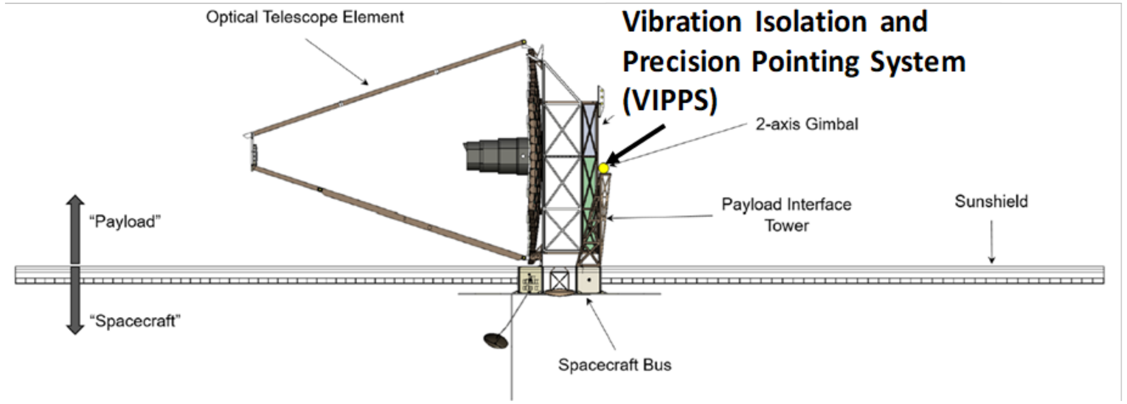

LUVOIR Architecture A (15 meter)

Specification	Value
Aperture diameter	15 meters
Field-of-View	15 arcmin x 8 arcmin
Static wavefront error	< 38 nm RMS
Pointing stability	+/- 0.3 mas (1σ) per axis over observations
WFE Stability	Picometer level; see subsequent charts
Object tracking	60 mas/sec
Slew rate	Req: repoint anywhere in anti-sun hemisphere in 45 minutes Goal: repoint anywhere in anti-sun hemisphere in 30 minutes

Vibration Isolation and Precision Pointing (VIPPS) control system

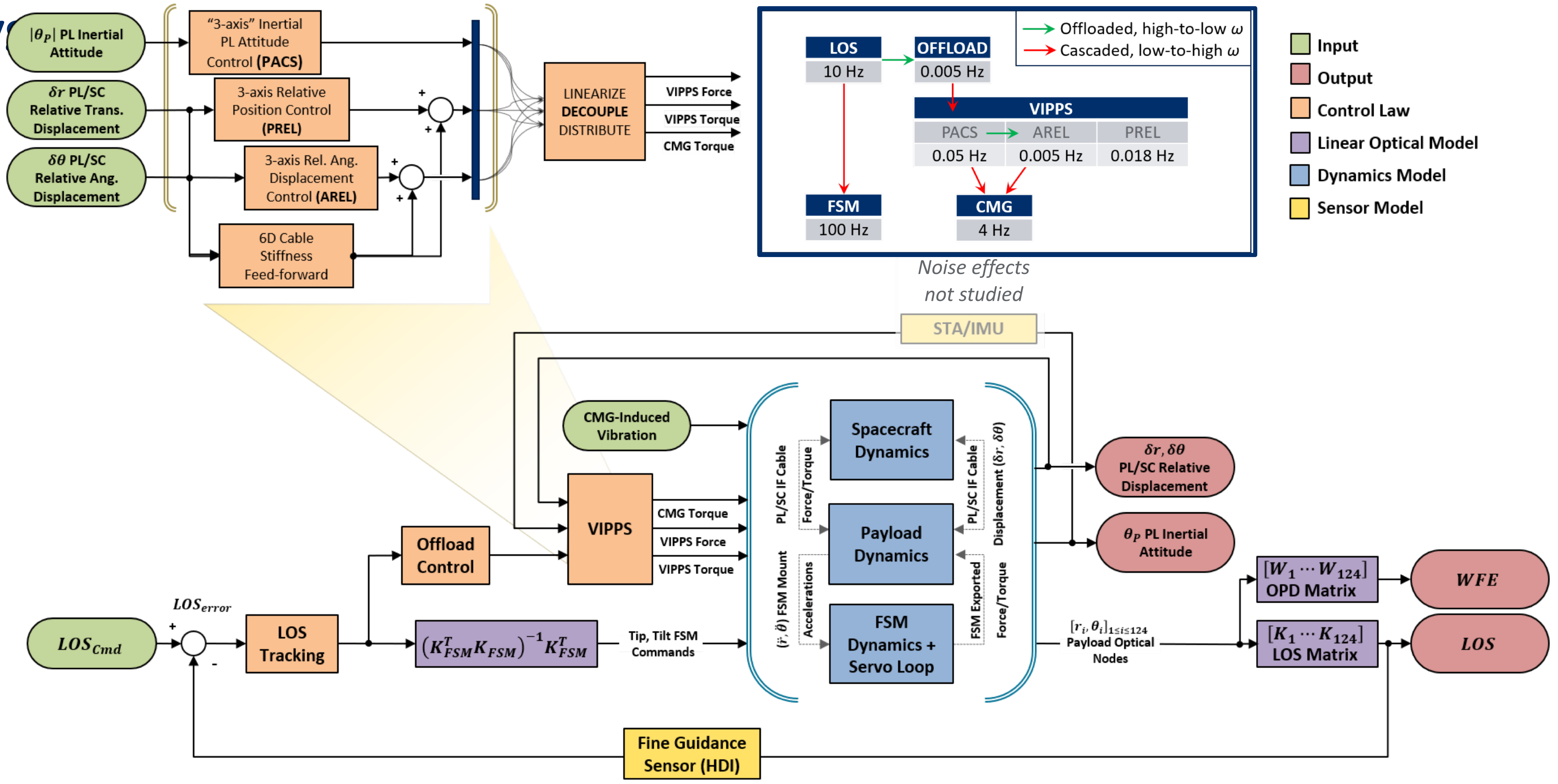

Actuator disturbance model development

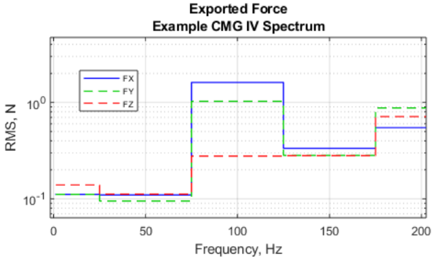

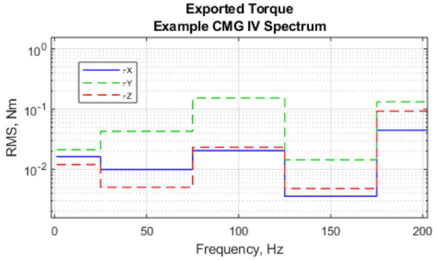

- Control Moment Gyro induced vibration
  - Disturbance profiles based on a set of four direct-drive CMGs, each having 217 N-m-sec nominal wheel momentum and a maximum gimbal rate capability of 0.4 rad/sec
  - For all 6DOF, the RMS of the spectrum was calculated in discrete frequency-bins: <25Hz, 25-75Hz, 75-125Hz, 125-175Hz, and >175Hz
  - Identical external load spectra were applied to each of four CMG nodes in the integrated system model in 8 randomized (but seeded) orientations for each integrated model
- Fast Steering Mirror (FSM) exported loads
  - Based on a FSM mechanical model from a recent flight development program, or comparable size needed for LUVOIR
  - Model assumed a momentum-compensated FSM design, with residual exported loads a function of the mismatch in mirror and reaction mass properties
- VIPPS non-contact actuator noise
  - Current in voice coil actuators assumed to be controlled by motor drive electronics with a high bandwidth current control system (RMS current noise of 50 micro-Amps per actuator, or 0.27 milli-Newtons RMS per-actuator)
- VIPPS electro-magnetic coupling

Interface cable coupling model

- Cable stiffness was modeled based on empirical data that was obtained from a testbed
- Testbed was instrumented to measure transmissibility of force and torque across cables of various configurations and geometries
- Analyzing transmissibility for all cable configurations suggested a constant stiffness matrix across the tested frequencies would be an accurate representation of the cable stiffness model
- An analysis was done to choose the maximum and minimum stiffness matrices over different cable configurations
- a proportional damping matrix was chosen such that the minimum modal damping for the 6 fundamental modes across the VIPPS interface is not lower than 0.005 (0.5%)

Table 5.1-5: Max and Min VIPPS Interface Stiffness Matrices

Maximum Stiffness Matrix	Minimum Stiffness Matrix
$\begin{bmatrix} \begin{bmatrix} 14.10 & 0.34 & 3.28 \\ 0.15 & 1.99 & 0.09 \\ 4.52 & 0.10 & 3.31 \end{bmatrix}_{[\mathrm{N/m}]} & \begin{bmatrix} 0.07 & 2.94 & 0.08 \\ 0.44 & 0.02 & 0.45 \\ 0.01 & 1.52 & 0.06 \end{bmatrix}_{[\mathrm{N/rad}]} \\ \begin{bmatrix} 0.13 & 2.08 & 0.08 \\ 13.76 & 0.27 & 3.93 \\ 0.24 & 1.31 & 0.03 \end{bmatrix}_{[\mathrm{Nm/m}]} & \begin{bmatrix} 0.56 & 0.04 & 0.44 \\ 0.05 & 3.71 & 0.09 \\ 0.25 & 0.03 & 0.56 \end{bmatrix}_{[\mathrm{Nm/rad}]} \end{bmatrix}$	$\begin{bmatrix} \begin{bmatrix} 1.69 & 0.02 & 0.35 \\ 0.03 & 0.17 & 0.01 \\ 0.45 & 0.01 & 0.42 \end{bmatrix}_{[\mathrm{N/m}]} & \begin{bmatrix} 0.01 & 0.51 & 0.01 \\ 0.05 & 0.02 & 0.05 \\ 0.01 & 0.30 & 0.01 \end{bmatrix}_{[\mathrm{N/rad}]} \\ \begin{bmatrix} 0.01 & 0.22 & 0.02 \\ 1.98 & 0.02 & 0.63 \\ 0.05 & 0.21 & 0.02 \end{bmatrix}_{[\mathrm{Nm/m}]} & \begin{bmatrix} 0.11 & 0.02 & 0.07 \\ 0.01 & 0.75 & 0.01 \\ 0.06 & 0.02 & 0.16 \end{bmatrix}_{[\mathrm{Nm/rad}]} \end{bmatrix}$

Note: unsigned stiffness values shown here

Sensor noise model development

- FSM servo control sensor noise
  - Jitter due to servo control sensor noise was also modeled (+/- 10 arc-sec range assumed, 17 bits effective resolution)
- High Definition Imager (HDI) LOS sensor noise
  - Study assumes that the HDI has a pixel Instantaneous Field of View (IFOV) of 2.75 mas/pixel
  - Measurement of the LOS error will involve centroiding on the regions associated with the target star (or stars)
  - Noise model assumed 1/10 pixel of RMS centroid noise per measurement, modeled as band-limited white Gaussian noise
- VIPPS non-contact sensor noise
  - Each non-contact sensor at the VIPPS interface was assumed to have a range of +/- 10 mm
  - Assuming an effective resolution of 19 bits, this implies a per-sensor RMS measurement error of 19 nm over the stroke
  - Measurement noise is modeled as band-limited white Gaussian noise

Linear optical model (LOM) development and integration

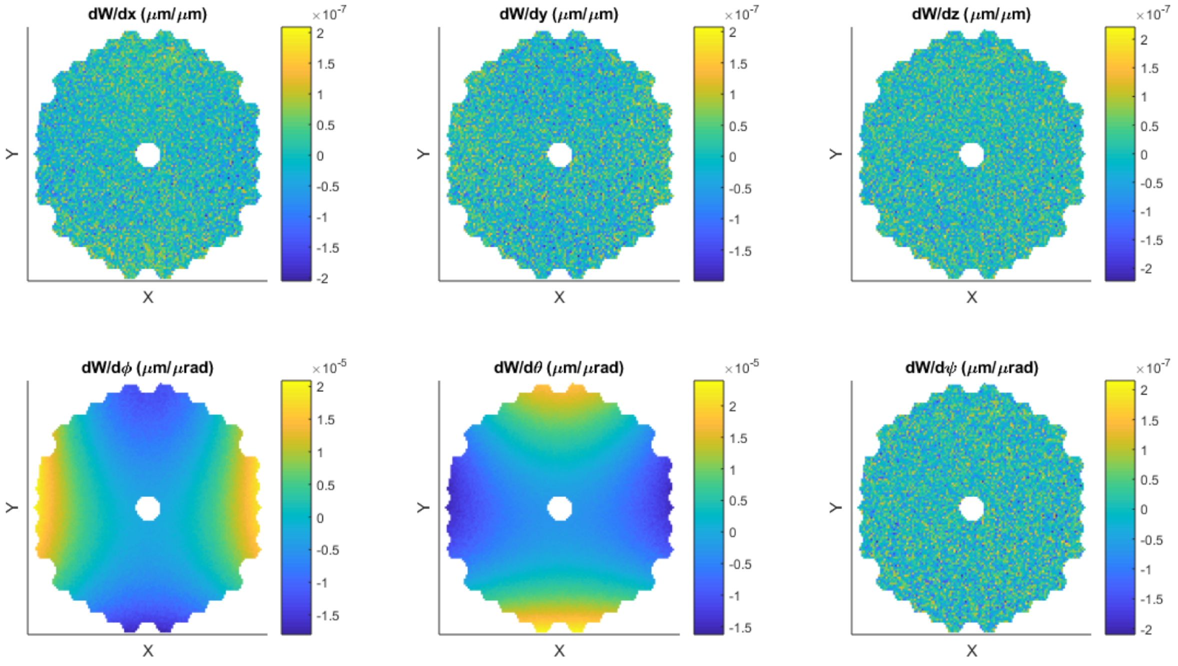

- Linear sensitivities captured the WFE contribution from the principal OTA optical elements (PM, SM, TM, FSM)
- WFE contributions due to instrument optics were not included
- Rigid-body checks of the segmented optical sensitivities were run to verify that predicted WFE is numerical noise for observatory DOFs that do not contribute to WFE (translation and observatory roll (see chart at left)
- Tip/Tilt WFE sensitivities used to model HDI LOS measurement

- WFE sensitivities produce a 128x128 grid of sampled WFE across the aperture
- Result is passed through a spatial filter to separate WFE into low-spatial frequency (< 1 cycle/segment) and high spatial frequency (>1 cycle/segment)
- The spatially decomposed WFE combines in an RSS sense to the overall WFE stability metric

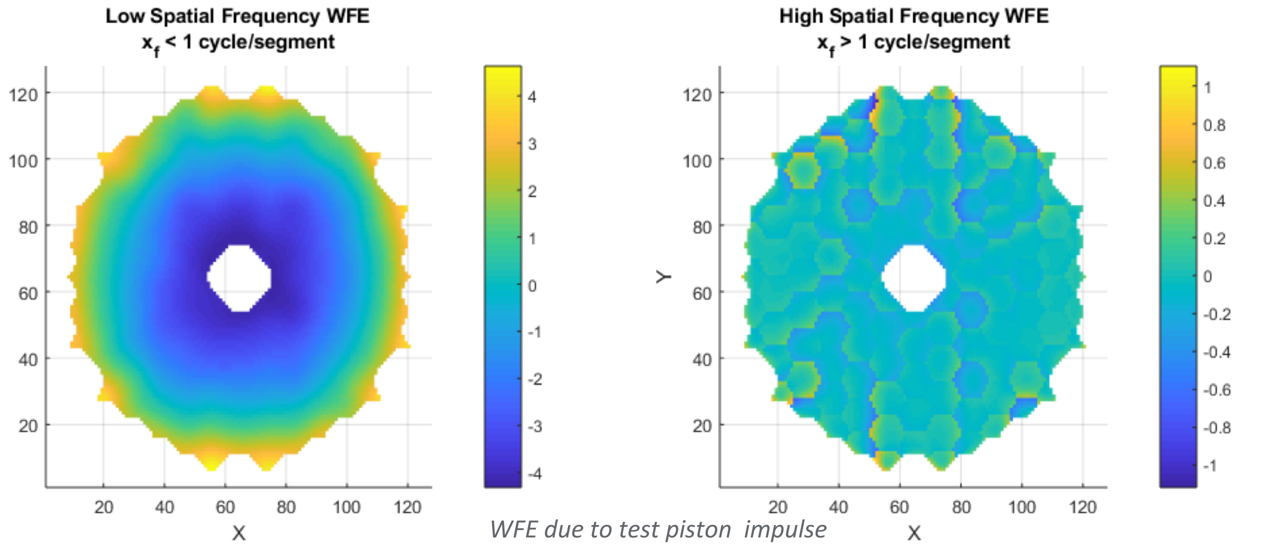

WFE due to test piston impulse response

Structural dynamics model development

- Structural dynamic model obtained from the LUVOIR Science and Technology Development Team (STDT)
  - The FEM is comprised of 51266 grid points and 61768 elements
  - Mass of the telescope and instrument portion is approximately 23128 Kg; mass of the spacecraft, including VIIPS, is 11490 Kg
- Structural models were synthesized for 6 different payload orientations and 2 different VIPPS cable stiffnesses (12 models)
- Dynamic WFE and LOS stability results presented in this section were computed over a frequency range of 0.05-200Hz
- Frequency-domain performance computed in overall and binned RMS, with bin fixed edges at: 0.1, 29, 57, 86, 114, 143, 171, and 200Hz

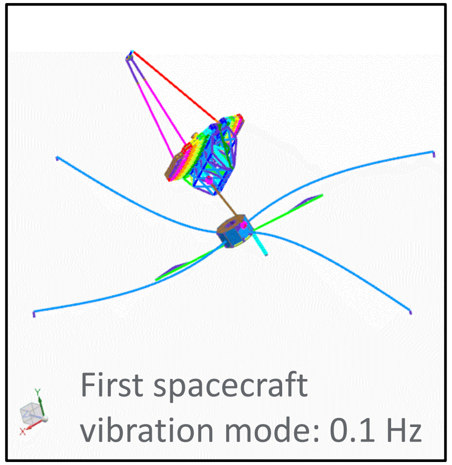

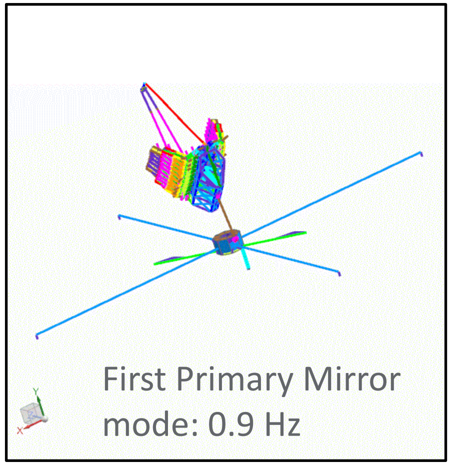

Animations of <u>separated</u> Payload and Spacecraft structural modes

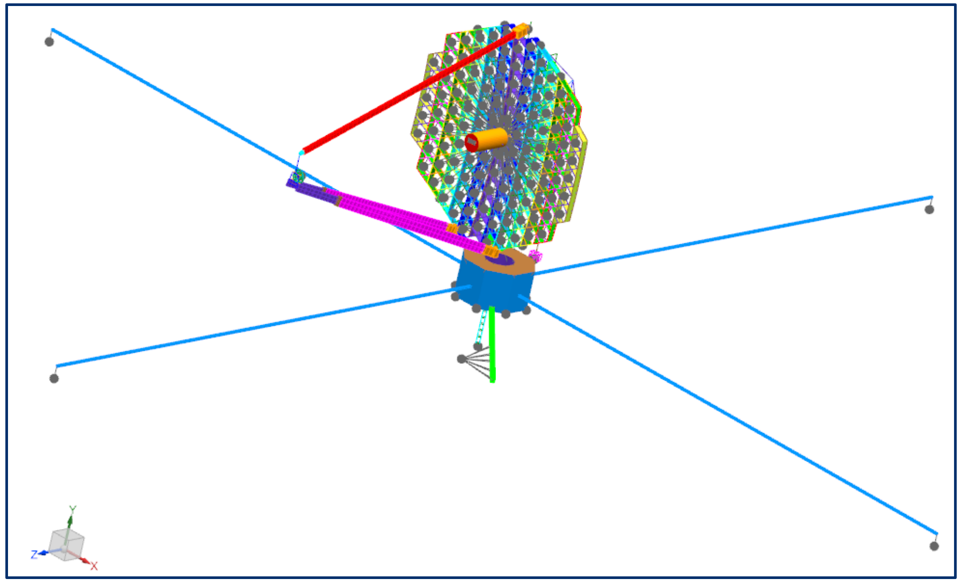

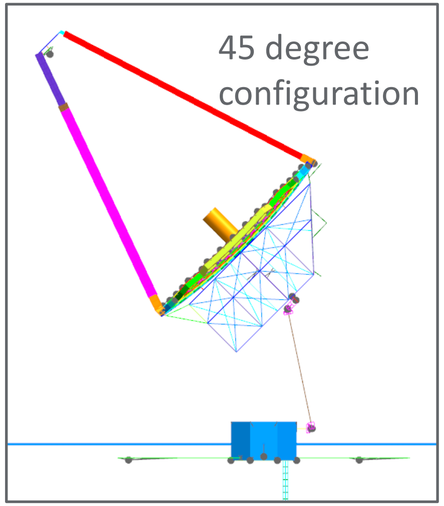

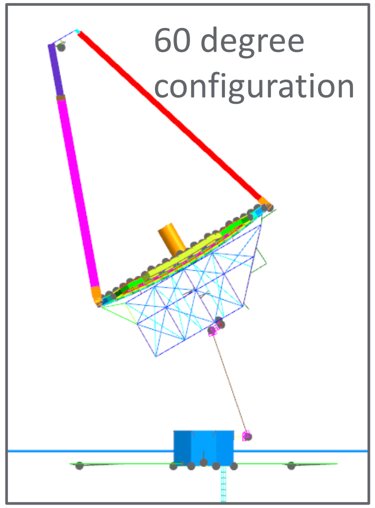

Spacecraft-to-Payload angular transmissibility

- Rigid-body transmissibility (left-side plots at right)
  - Open-loop system shows 0 dB transmissibility due to cable coupling
  - Addition of Payload attitude control results in disturbance rejection bandwidth of ~0.01 Hz
  - FSM boosts disturbance rejection bandwidth to ~10 Hz
- Flexible-body transmissibility (right-side plots at right)
  - Same trends as rigid-body model at low frequency
  - Flex effects show peaking at high frequency due to payload dynamics

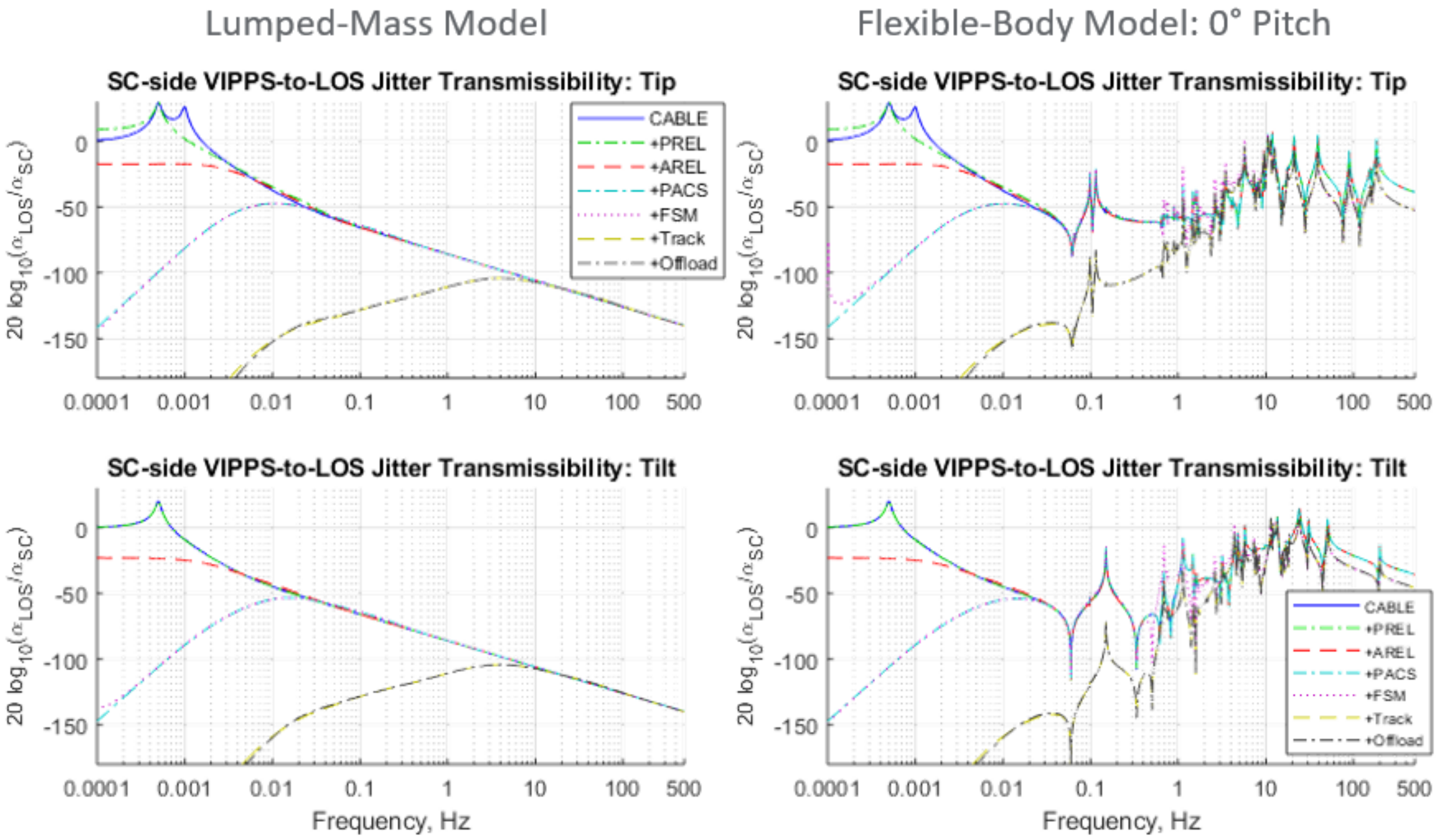

LOCKHEED MARTIN

LOS error power spectrum performance: baseline control syst

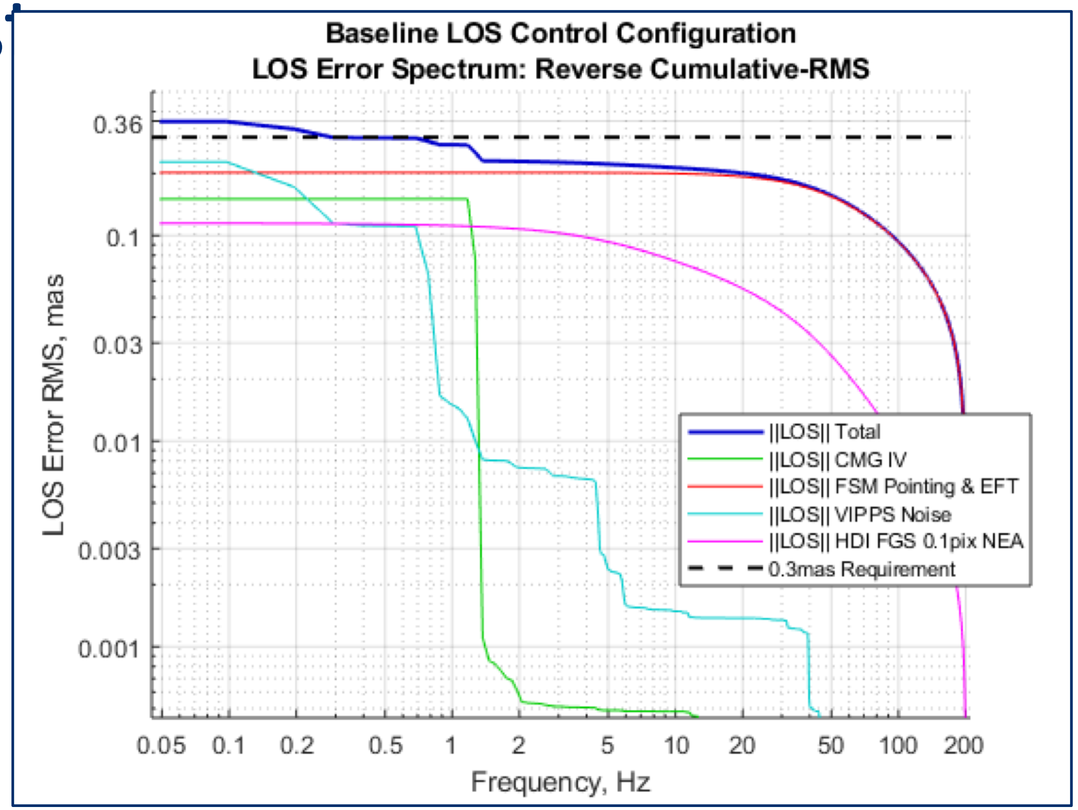

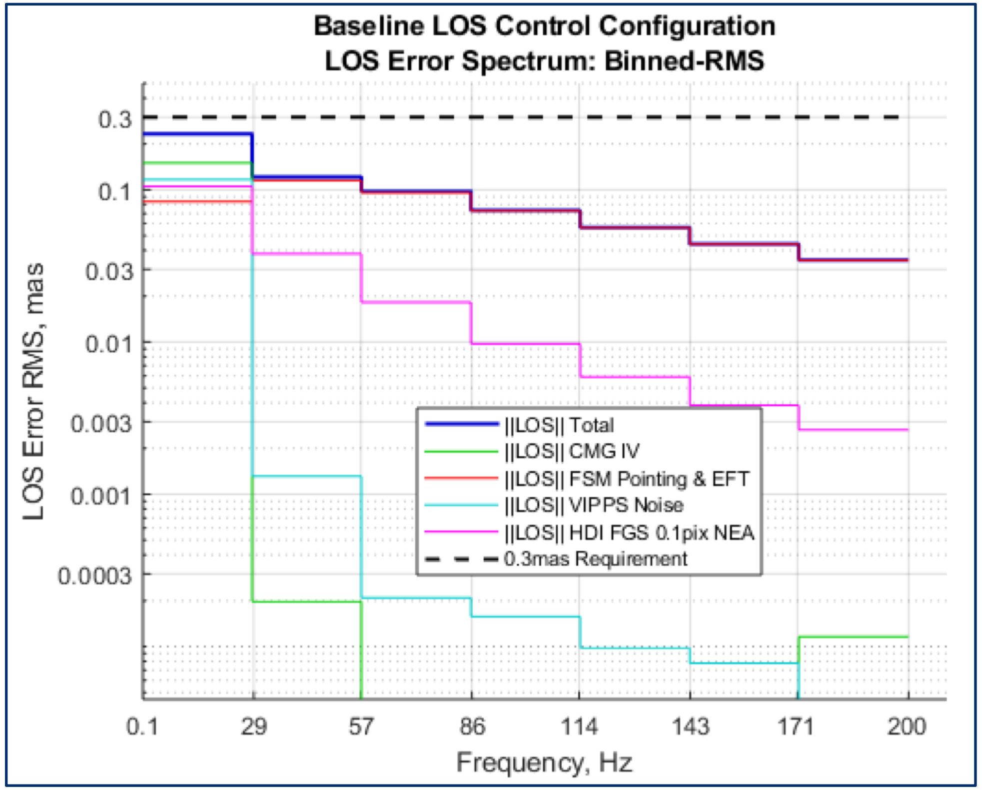

Reverse-cumulative RMS (left) and binned RMS (right) LOS error for worst-case structural dynamic model; different noise sources are activated to compare the relative contribution of each; performance slightly exceeds 0.3 mas requirement, but compliance can be recovered by reducing FSM servo control bandwidth

Wavefront error power spectrum: baseline control system

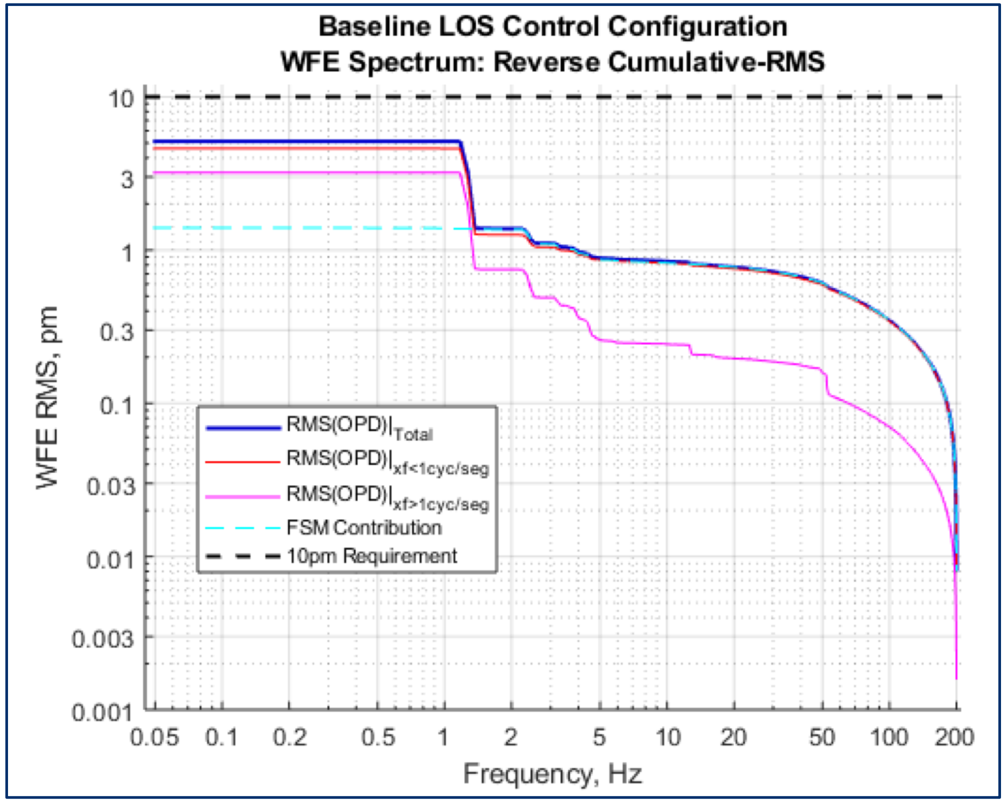

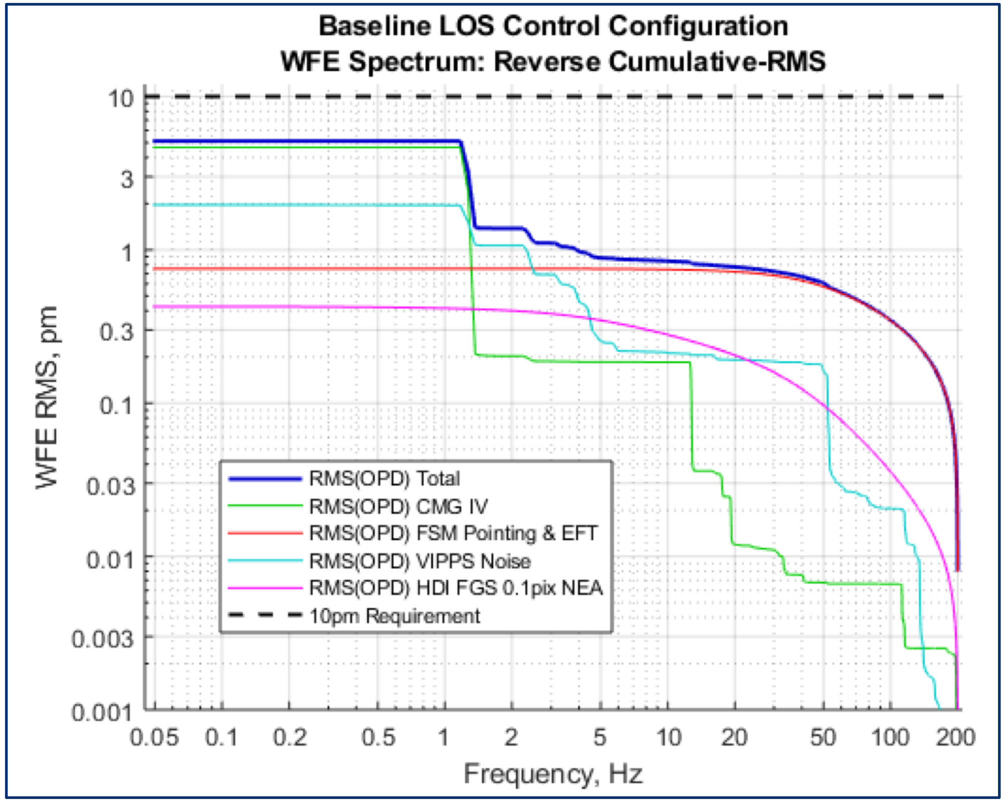

Reverse-cumulative RMS separated in two spatial frequency bins (left) and by error source (right) WFE for worst-case structural dynamic model; different noise sources are activated to compare the relative contribution of each; compliance with a nominal 10 pm RMS WFE requirement is predicted

LOS error power spectrum: performance without FSM

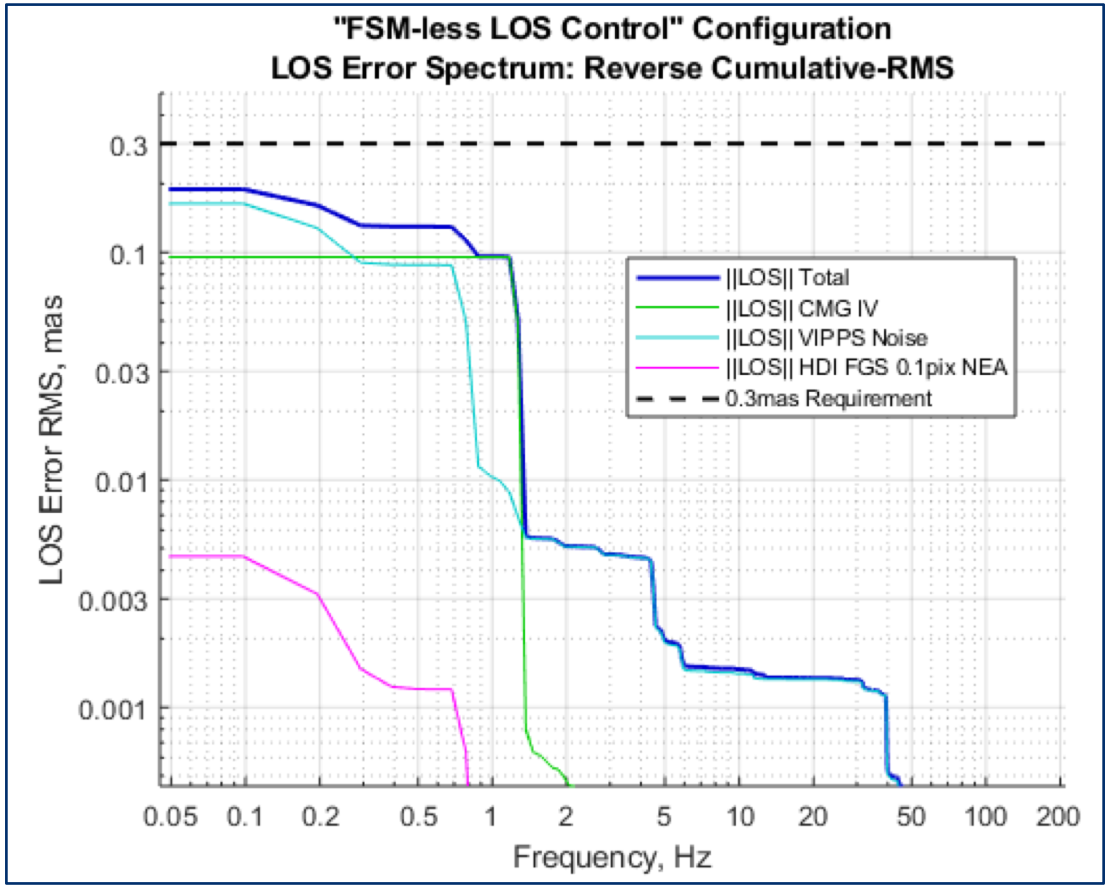

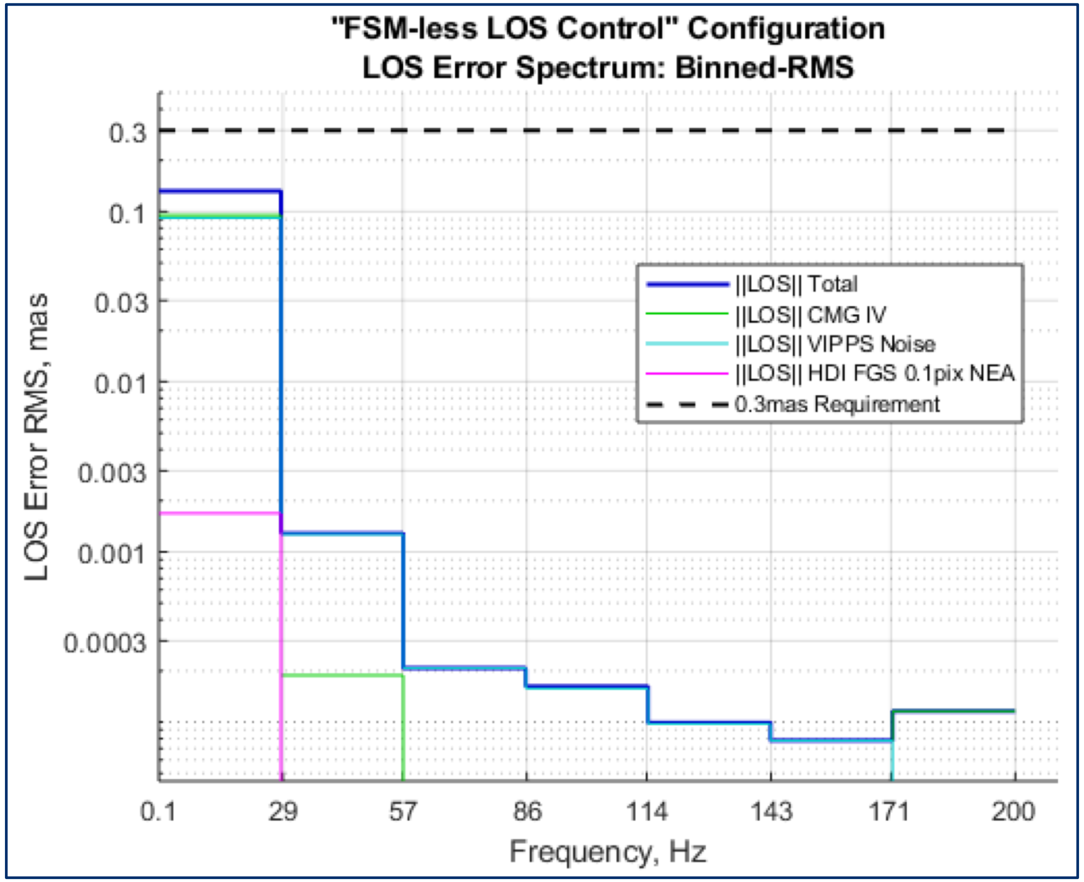

Reverse-cumulative RMS (left) and binned RMS (right) LOS error assuming no FSM in control system; compliance to LOS error is predicted with margin

Wavefront error power spectrum: performance without FSM

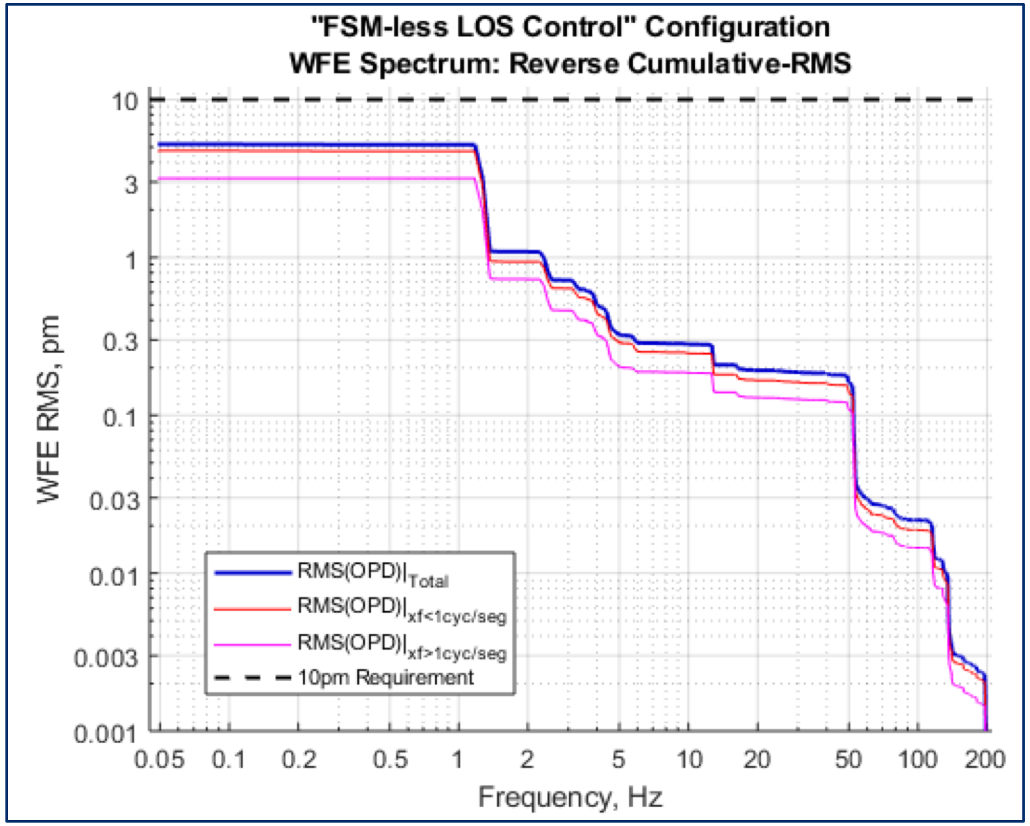

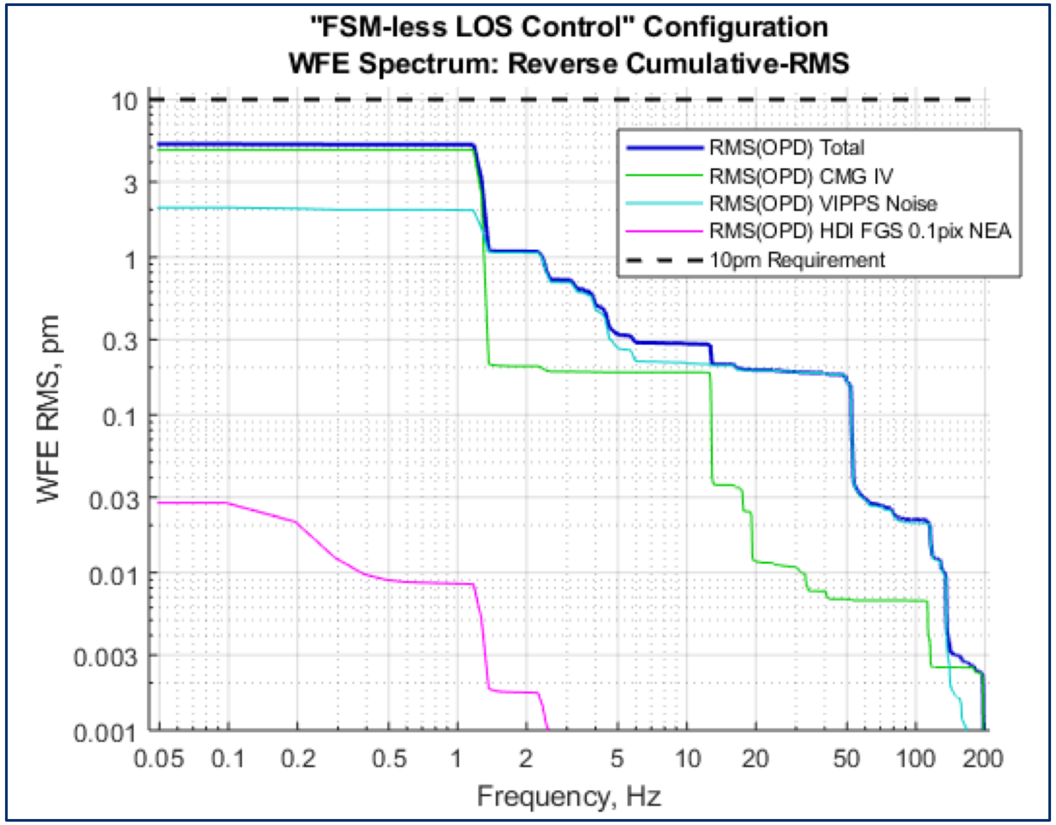

Reverse-cumulative RMS separated in two spatial frequency bins (left) and by error source (right) WFE assuming no FSM in control system; WFE performance is not appreciably altered by presence or absence of FSM

Dynamic WFE stability error budget: anchored to end-to-end models

Spatial frequency bins	Low Spatial (< 1 cycle/segment)						High Spatial (> 1 cycle/segment)					
Temporal frequency bins (Hz)	< 1		1 - 10		> 10		< 1		1 - 10		> 10	
	Alloc	Perf	Alloc	Perf	Alloc	Perf	Alloc	Perf	Alloc	Perf	Alloc	Perf
Actuator Effects	**2.9**	**0.2**	**4.5**	**4.1**	**1.1**	**0.2**	**1.4**	**0.1**	**5.2**	**2.9**	**1.1**	**0.2**
CMG induced vibration	1.00	0.00	4.00	3.80	1.00	0.15	1.00	0.00	5.00	2.68	1.00	0.11
Fast Steering Mirror exported loads	N/A	Modeled	N/A	Modeled	N/A	Modeled	N/A	Modeled	N/A	Modeled	N/A	Modeled
VIPPS non-contact actuator noise	2.50	0.19	2.00	1.57	0.50	0.17	1.00	0.07	1.50	1.14	0.40	0.13
VIPPS electromagnetic coupling	N/A	Modeled	N/A	Modeled	N/A	Modeled	N/A	Modeled	N/A	Modeled	N/A	Modeled
Gimbal mechanism actuator noise	1	TBD	0.2	TBD	0.1	TBD	0.2	TBD	0.2	TBD	0.2	TBD
Sensor Effects	**0.5**	**0.1**	**1.0**	**0.3**	**1.4**	**0.8**	**0.5**	**0.0**	**0.3**	**0.1**	**1.0**	**0.2**
Fast Steering Mirror servo control sensing error	0.05	0.00	0.20	0.11	1.00	0.73	0.05	0.00	0.30	0.02	1.00	0.15
HDI LOS sensing noise	0.05	0.10	1.00	0.30	1.00	0.27	0.05	0.02	0.10	0.06	0.10	0.05
Payload attitude reference sensing noise	0.5	TBD	0.1	TBD	0.05	TBD	0.5	TBD	0.1	TBD	0.05	TBD
VIPPS non-contact sensing noise	0.1	0	0.1	0	0.1	0	0.1	0	0.1	0	0.1	0
TOTAL (by column)	**2.9**	**0.2**	**4.6**	**4.1**	**1.8**	**0.8**	**1.5**	**0.1**	**5.2**	**2.9**	**1.5**	**0.2**
TOTAL (Performance)	**5.13**											
REQUIREMENT	**10**											
TOTAL MARGIN (Performance)	**49%**											
TOTAL MARGIN (Allocation)	**19%**											

LUVOIR transient stability study: LOS and WFE settling after slew maneuver

- To perform its mission, LUVIOR is required to meet requirements on repositioning of the observatory over a hemispherical field-of-regard
- During slew, the observatory experiences a different disturbance environment, including flexible body modes coupling into rigid-body degrees of freedom, and Control Moment Gyro Output Torque Ripple (OTR)
- To initial investigate the expected settling time, a restricted slew maneuver of the entire observatory about the sunline (i.e., no pitch maneuver of the telescope) over a small angular range of 5 degrees
    - Small angular range was necessary to maintain the linearity assumption in the linear structural dynamics model
    - However, the full agility afforded by the CMGs and the VIPPS actuators, and the minimum angular rate (0.09 deg/sec) to support the hemispherical repositioning requirements were exercised in this restricted 5-deg slew (see profiles at right)

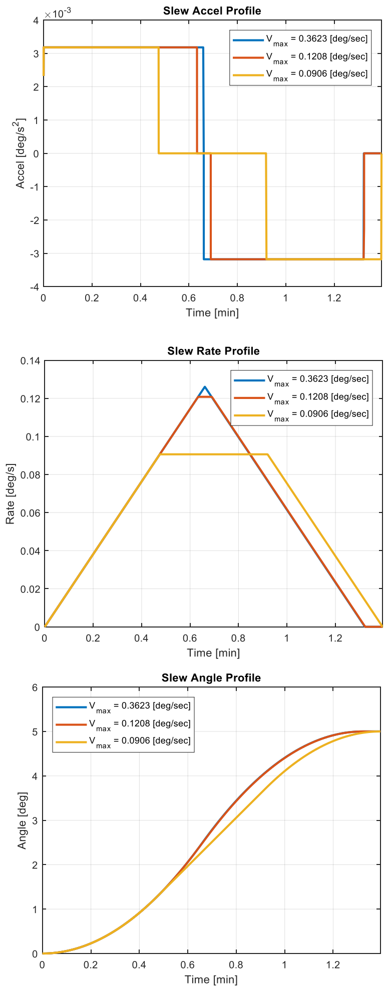

VIPPS control architecture assumed during slew

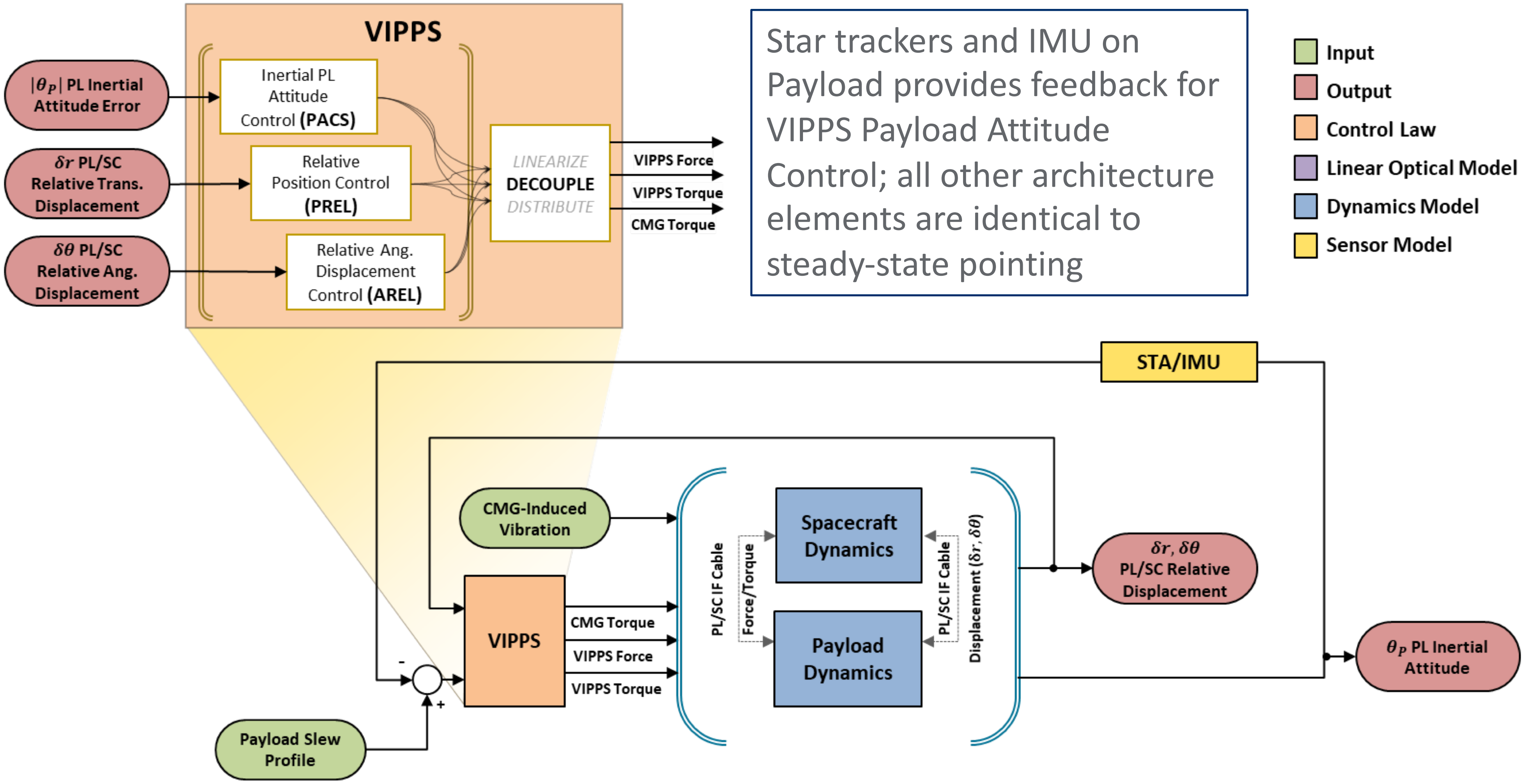

Star trackers and IMU on Payload provides feedback for VIPPS Payload Attitude Control; all other architecture elements are identical to steady-state pointing

- Input
- Output
- Control Law
- Linear Optical Model
- Dynamics Model
- Sensor Model

Example results: LOS and WFE settling performance

Note: results shown here are for 0 deg. payload pitch angle (worst-case configuration)

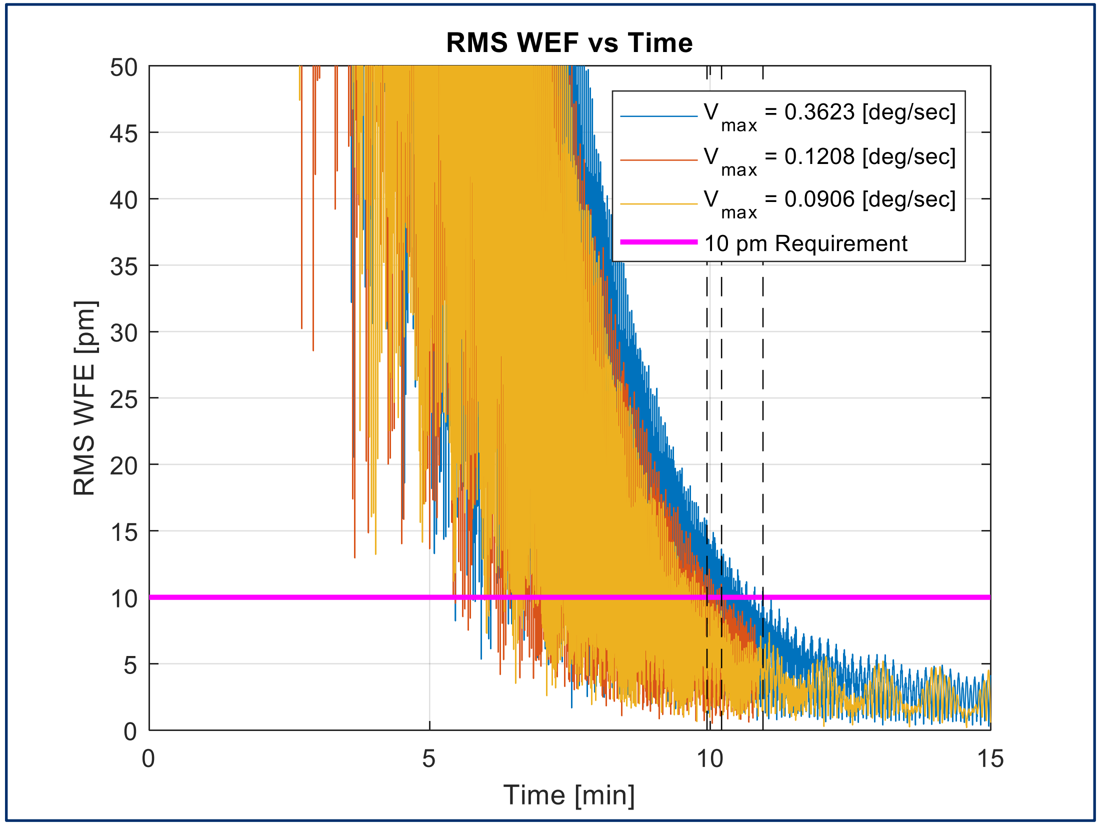

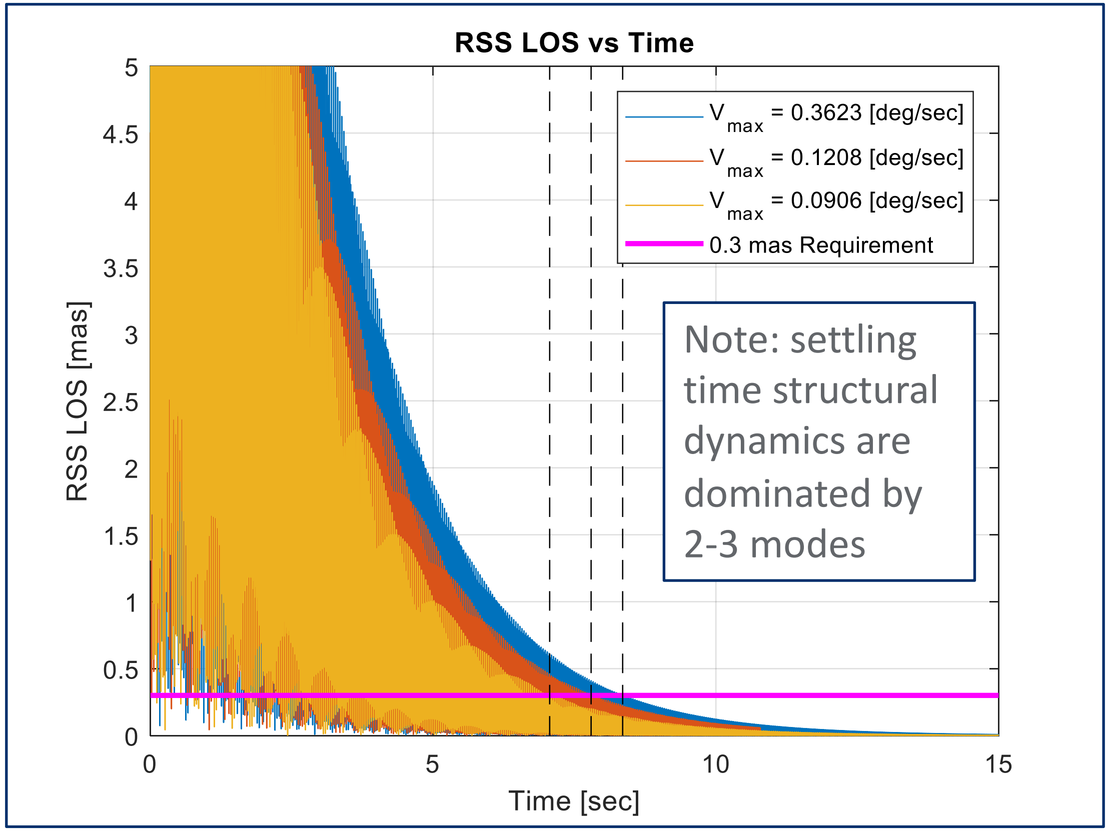

The plots above show RMS WFE (left) and Root-Sum-Square (RSS) of LOS error after slew completion (horizontal axis is time since slew end); results show that over a broad range of maximum slew velocity (greater than required min rate of 0.09 deg/sec) settling time is less than about 10 minutes

Summary of key findings: end-to-end dynamic stability modeling

- The line-of-sight (LOS) and wavefront error (WFE) dynamic stability requirements for the 15-meter LUVOIR architecture can feasibly be met with a non-contact vibration isolation and precision pointing system (VIPPS)
- a FSM does not appear to be necessary to meet the LUVOIR dynamic stability requirements for LOS and WFE stability.
  - A FSM may be needed to support other instrument operations of the observatory concept of operation in general; this study underscores the importance of carefully specifying the bandwidth and noise characteristics of the FSM
- Transient settling time of the LOS and WFE for the 15-meter LUVOIR architecture is estimated to be on the order of 5-10 minutes, depending on the design parameters of the slew and the slew agility
  - Restricted study only looked at single-axis slew maneuvers over a small angular range, but executed the entire needed agility envelope for LUVOIR

THIS STUDY ILLUSTRATED THE IMPACT AND IMPORTANCE OF RIGOROUS END-TO-END MODELING OF LARGE, SEGMENTED OPTICAL SYSTEMS

Suggested next steps: end-to-end dynamic stability modeling

- Expand spatial and temporal fidelity of integrated modeling and frequency domain disturbance models to cover a broader and higher sampling
  - Lower frequency to capture long-period dynamic LOS and WFE stability
- Model nonlinear optical sensitivity effects, or at least estimate the impact of neglected higher-order effects in optical models
- Develop a nonlinear flexible body dynamic model to better assess the dynamic stability settling time over large angles and with 2-axis gimbal degrees of freedom

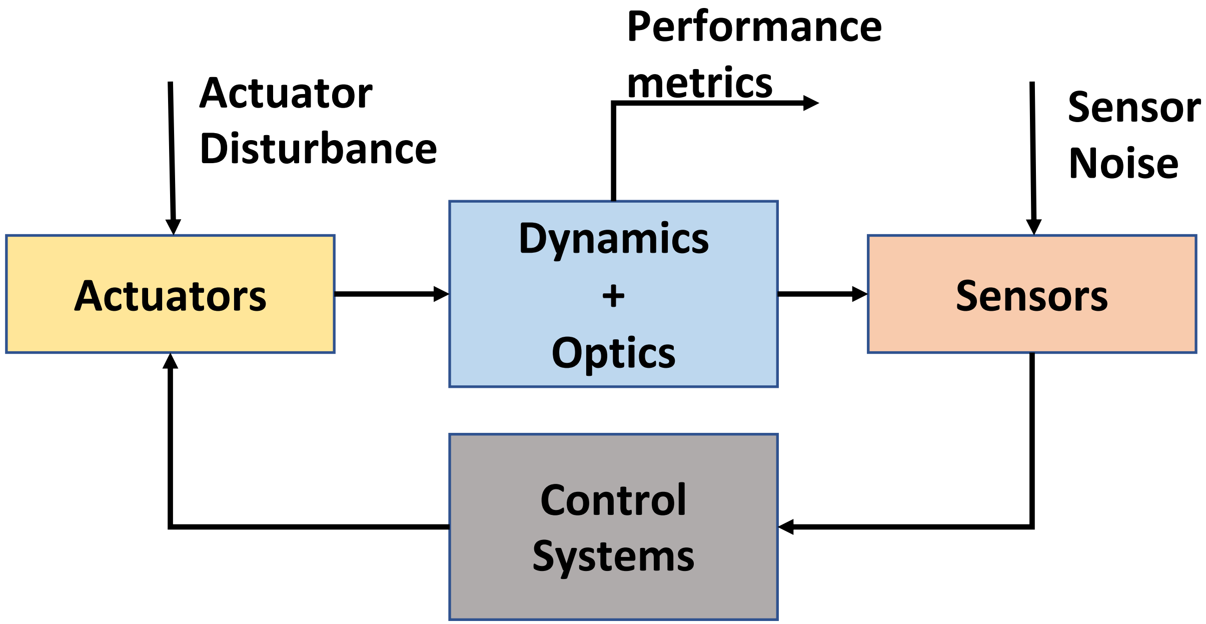

LOCKHEED MARTIN